Modeling of pulsed Laser Thermal Annealing for junction formation optimization and process control

R. Negru, K. Huet, P. Ceccato, B. Godard

Excico, 14 rue Alexandre, 92230 Gennevilliers, France

Abstract

It is now a well-known that the next generation devices in many fields of the semiconductor industry will be based on 3D architectures. In this framework, low thermal budget annealing technological solutions are required. For many applications, either in the field of sensors, microprocessors or high density memories, the Laser Thermal Annealing (LTA), an ultrafast and low thermal budget process, is one of the most promising solutions. This UV (308nm) pulsed laser annealing process has already been adopted in production for the passivation step of BackSide Illuminated CMOS Imaging Sensors, and the contact formation step of Power devices. During the annealing process, the high temperature region (e.g. over 1400°C) needs to be restrained to very thin layers (from nm to µm range) while keeping of the underlying fragile layers (metal, bonding) and devices at low temperature (e.g. less than 300°C).

In order to offer appropriate annealing solutions to the recent developments in 3D architectures, an accurate modeling of the LTA process is needed. In this work, the modeling of this ultra low thermal budget process is detailed. The results show an excellent agreement with experimental data and allow quantifying equipment induced process variability.

1. INTRODUCTION

Laser Thermal Annealing (LTA) is a technique for junction formation in process fabrication of semiconductor devices. It enables high activation and low surface roughness. It is an ultrafast process (few µs) with the ability to provide a low thermal budget to melt locally the crystalline Silicon (c-Si) without damaging the stacked layers. In the framework of implanted dopants annealing, the LTA process results in box like profiles [1],

EXCICOLTA laser source is based on $(XeCl)^*$ diplex desexcitation under electrical discharge towards fundamental level (see Figure 1). Into c-Si the absorption is realized within the first 7 nm and the melting temperature is reached in few tens of ns. The pulse duration (PD) is of ~150ns and it provides high energy density (ED), e.g. up to 3J/cm^2 for a beam size of 20x20mm^2. Silicon melt depth (MD) reached during LTA process depends on PD and ED [1-6].

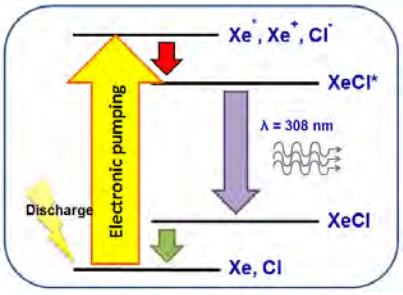

Fig. 1. *Laser pulse formation by dissociation of* $(XeCl)^*$.

One of the excimer laser technology challenge is the pulse duration stability. LTA process depends on: gas (mix, temperature, ionization[1], and aging), electrical discharge and optical path fouling. A set of procedures were defined to maintain the optimum conditions for the process. So, as the gas ages, in order to maintain the same energy deposited on the sample, the excitation energy increases. Preventive maintenance procedures are used to maintain a clean optical system. As for the quality of the gas, a gas purifier loop (GPL) is used to trap all the impurities. ED is measured at sample surface level after all losses in the optical path. PD and melting time (MT) are two other physical parameters that can be measured during the process.

In order to adapt and control the LTA process, the user disposes of two main parameters:

- ⇨ electrical discharge (furnished by a capacity banc)[2]
- ⇨ gas mix (others are constructive and are not subject of this study).

The impact of these parameters on LTA process can be translated in a PD change and in an ED shift.

The semiconductor industry provides a large panel of applications for the LTA equipment (e.g. image sensors, power devices, logic, 3D TSV, memories or MEMS). Each application has specific requirements depending on its own design and process flow. Usual application requirements are based on physical parameters that cannot be measured in-situ during LTA process, such as the junction depth (related to MD) or the maximum allowed temperature at a given interface

A need for process simulation that correlates the laser parameters with the applications key requirements is identified.

In this article, we present the model developed for LTA process of c-Si. This study is focused on evaluating the model validity and accuracy for changes in critical LTA source parameters (PD and ED). The model is based on a finite element specific system of equations and was

[1] Ionization is necessary to make a uniform discharge

[2] Population inversion with fundamental level

implemented using the simulation software environment COMSOL Multiphysics, which provides a powerful solver tool and enables the possibility to specify your own partial differential equations system (PDE) and link them with other equations or physics. The simulation results are compared to reference experiments.

2. MODEL

LTA process simulation requires modeling the temporal and spatial evolution of the temperature in the device, liquid layer formation and its recrystallization, as well as dopant redistribution after process.

Through multiple approaches that are available into literature we resumed to Phase-Field method to simulate the temperature behavior and the liquid layer formation [7]. Because the Boron profiles show depletion near silicon surface and a build-up at the initial liquid/solid interface in silicon we choose to implement the Adsorption as physical mechanism [8-9].

Thus, COMSOL Multiphysics provides us finite element analysis software that enables us to solve three PDE: a. Heat equation, b. Phase-Field equation and c. Diffusion-segregation equation.

2.1 Phase-Field approach

The Phase-Field approach [7] uses a continuum phase φ formalism (with -1 ≤ φ ≤ +1, where φ = -1 symbolizes pure liquid and φ = +1 is for pure solid phase). The Heat (1) and the Phase-Field equations (2) are solved together:

$$\rho C_p \frac{\partial T}{\partial t} - \nabla^2(KT) = \frac{\rho L_{fus}}{2}\frac{15}{8}(\varphi^2-1)\frac{\partial \varphi}{\partial t} + S(x,t) \quad (1)$$

$$\tau \frac{\partial \varphi}{\partial t} = W^2\nabla^2\varphi - \varphi(\varphi^2-1) - \lambda\frac{C_p}{L_{fus}}(T-T_M)\cdot \cdot (\varphi^2-1)^2 \quad (2)$$

where the material properties are represented by density ρ, heat capacity C_p and thermal conductivity K. Those parameters are phase and temperature dependent. L_{fus} is the latent heat of crystalline silicon. $\frac{15}{8}$ is a normalization factor. T_M is the silicon melting temperature. τ, W and λ are the Phase-Field equation parameters and represent the thermal relaxation time, the thickness of the phase transition layer and the coupling parameter between the phase and heat diffusion, respectively.

In the heat equation the left side terms includes the latent heat source, and the external heat source:

$$S(x,t) = E_{las}P(t)(1-R)\alpha e^{-\alpha x} \quad (3)$$

where E_{las} is the incident laser fluency, $P(t)$is the laser pulse shape, R and α are the phase and temperature dependent surface reflectivity and the material absorption at the wavelength.

During the LTA process we have access to 3 main experimental results: ED, PD and MT. Other data such as MD or surface temperature (T_{surf}) cannot be measured in-situ, but they can be extracted from model simulations.

Tab. 1. *Thermal and optical material (c-Si) parameters used in LTA process simulations [11-12].*

Parameter		Value	Units
ρ	sol liq	2.32 2.52	g/cm^3
C_p	sol liq	$10\cdot T^{1.034/(1.02-0.01\cdot T)}-213$ 1045	J/kg/K
K	T≤1200K T>1200K	$1523.7\cdot T^{-1.226}$ $9\cdot T^{-0.502}$	W/m/K
R	sol liq	$59+6\cdot10^{-3}\cdot T$ 78	%
T_M		1690	K

2.2. Adsorption physical mechanism

The shape of the Boron profile obtained after LTA process cannot be explained by Fickian diffusion [9]. The typical profile shape shows depletion near the silicon surface and a build-up near the maximum melt depth. You et al. in [9] developed a diffusion-segregation equation based on adsorption physical mechanism, is:

$$\frac{\partial C_B}{\partial t} = \nabla(D_B\nabla C_B) - \nabla\left(D_B\frac{C_B}{C_{equ}}\nabla C_{equ}\right) \quad (4)$$

C_B and D_B denote the concentration and diffusion coefficient of Boron, respectively. D_B is temperature and phase dependent.

In equation (4) the first term on the right-hand side describes Fickian diffusion. The second term is used to describe the segregation of the Boron atoms. In the steady state, the dopant concentration in the vicinity of liquid/solid interface is proportional to the equilibrium concentration C_{equ} and the right-hand term vanishes. C_{equ} is a non-dimensional parameters and represents the "hanging" of the dopant to liquid/solid interface. From Hackenberg et al. [8], we can set C_{equ} to unity in the liquid, 0.8 in solid and 2.8 in the interface region between liquid and solid.

Tab. 2. *Boron diffusion-segregation parameters [8].*

Parameter		Value	Units
D_B	sol liq int	$0.002\cdot10^{-4}$ $2.2\cdot10^{-4}$ $1.8\cdot10^{-11}$	cm^2/s
C_{equ}	sol liq int	0.8 1 2.8	-

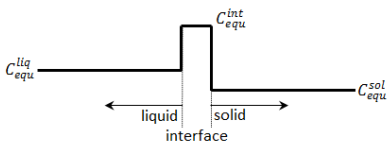

Fig. 2. Shape of the equilibrium concentration used for the simulation of adsorption.

3. DESIGN OF EXPERIMENTS

In order to evaluate our experiments we take as target the applications requirements in terms of MD. So, in this specific study, we chose for ED a range between 1.4 J/cm^2 (sub-melt or threshold, depends on PD) and up to 3 J/cm^2. As for PD, the targeted variability was between 130 ns and 160 ns. In the following we limited it to three values (135 ns, 145 ns and 155 ns). The corresponding pulse profiles used are reproduced in Figure 3.

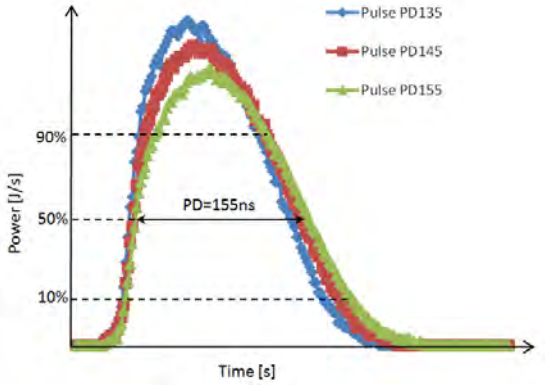

Fig. 3. *Temporal shape of laser beam and measure of PD.*

Surface melting time (MT) of the silicon is monitored in real time by measuring the reflectivity variation at 635 nm of exposed area.

The melting depth cannot be estimated in-situ, so a common approach for MD extraction is to analyze the dopant diffused profile after LTA as compared to the as-implanted one (not annealed). The reference experiments samples consist of 2 Boron implanted n-type (100) bulk Si wafers with 32 Ω·cm resistivity. Boron implantation was performed at energy of 3 keV and a dose of 5 x 10^{14} cm^{-2} for the first set of samples and 30keV with a dose of 1 x 10^{15} cm^{-2} for the second set. It is essential to consider two different dopant profiles, one deep (30 keV case) and one shallow (3keV case). Indeed, shallow implanted samples allow a more accurate melt depth extraction at low ED and deep implant are better suited for high ED conditions. MD is estimated from SIMS[3] profiles as depicted in Figure 4[4].

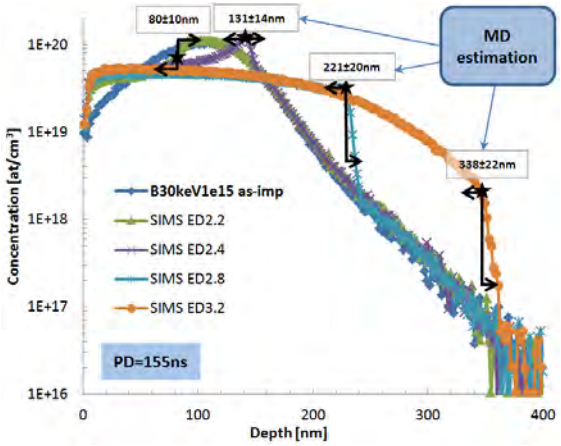

Fig. 4. *SIMS profiles for B$^+$ 30keV 1 x 10^{15} cm^{-2} and MD estimation. We notice that at lower ED (<2.2J/cm^2) is difficult to estimate de MD, and as ED increases (>3J/cm^2) the MD estimation error increases and the junction loses its sharp profile.*

4. RESULTS AND DISCUSSIONS

4.1 Phase-change model prediction

From SIMS profiles we have extracted, for PD values of 135, 145 and respectively 155 ns, the MD at various ED from 1.4 to 3.0 J/cm^2. In this range the experimental ED stability was within ±3%. Solving the systems of equations presented in 2.1 section for each PD pulse, we obtained the model response. It can be noticed from Figure 5.a that for a given ED, MD increases when PD is reduced. The model reproduces the observed experimental trends with an accuracy over 96% (R^2)[5].

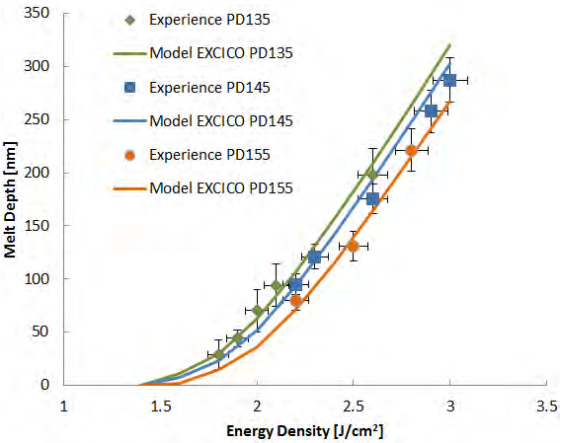

Fig. 5. *Experience and model for MD(ED) shift with PD*

The second process parameter analyzed was the melting time, MT. It can be measured and simulated. MT experimental deviation is around

[3] SIMS : Secondary Ion Mass Spectrometry

[4] SIMS error: ±5% in depth and ±10% in concentration

[5] R^2 : determination coefficient

5%. As shown on figure 6, the MT deviation with PD is not as significant and the MD variation observed earlier. The model accuracy is over 92%.

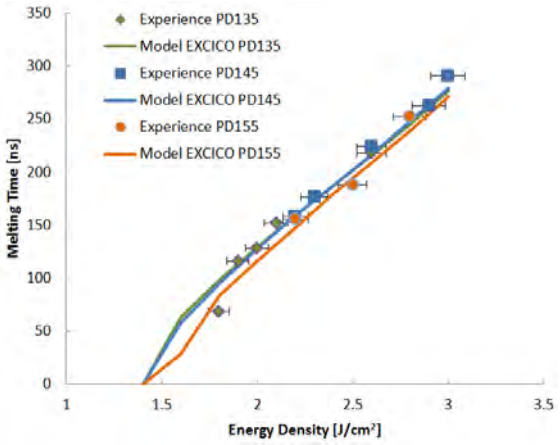

Fig. 6. *Experiment and model for MT(ED) shift with PD.*

At lower ED (around threshold) it is difficult to estimate MD, and the measurement of MT is limited by the system sensitivity. In this specific case, the model accuracy is difficult to evaluate. However, in the range of usual production utilization, the model reproduces with a reasonable precision, over 96%, the experimental trends.

4.2 Dopant diffusion and segregation model

In order to validate the observations made on SIMS measurements, we developed the diffusion-segregation model, already presented in 2.2 section. A model analyze was done for all three PD.

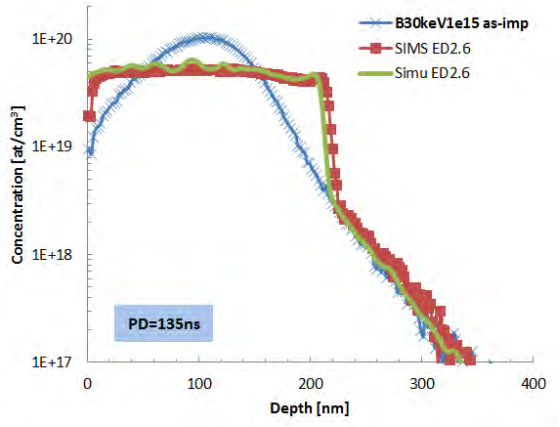

(a)

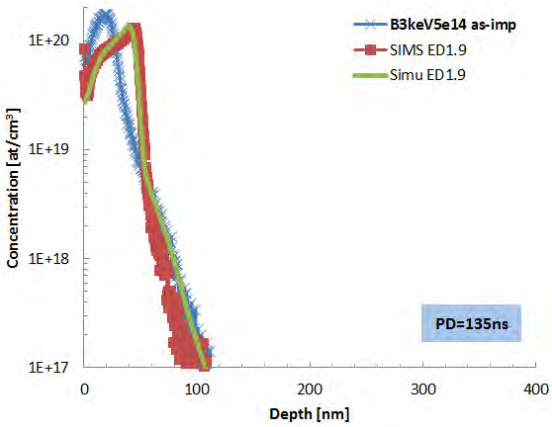

(b)

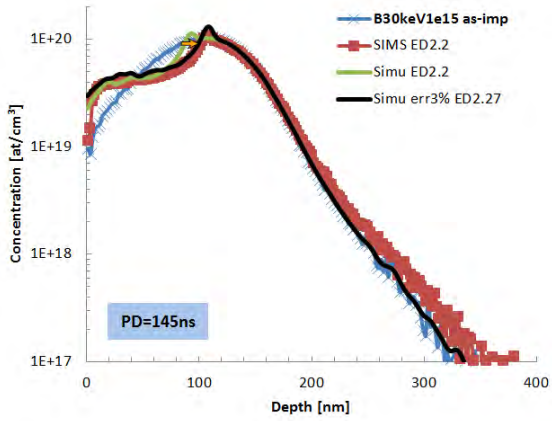

(c)

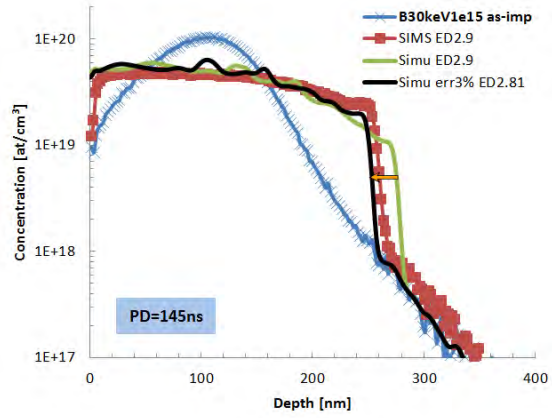

(d)

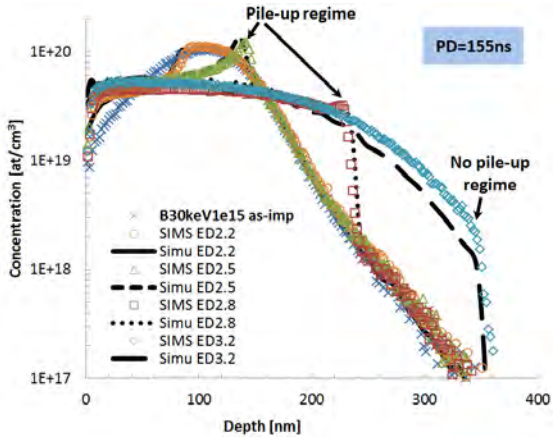

(e)

Fig. 7. *Measured SIMS profiles and simulated ones for (a-b) PD=135ns, (c-d) PD=145ns and (e) PD=155ns.*

In Figure 7.a-b the PD analyzed was 135ns. The B simulated profiles are very similar to measured one; the accuracy is 96% in (a) and 93% (b). The lower accuracy for the (b) case is essentially due to the SIMS measurement deviation in the implantation tail in non-melt region. The model is valid also for different implant conditions.

In Figure 7.c-d, an ED deviation of 3% was computed in order to study the model precision with process variability. The ±3% ED variation was enough to reproduce the experimental SIMS profiles.

In Figure 7.e we notice that Boron presents a pile-up phenomenon, where at the solid/liquid interface the dopant concentration overcome the implanted one. The cause is the adsorption phenomenon explained in section 2.2. We notice that this phenomenon disappear at higher ED, because the melt front and the Boron diffusion velocities are different.

So, considering normal variations for ED, the model is able to reproduce the experiences with a good accuracy over 90%.

5. CONCLUSIONS

In this study, it was demonstrated that the phase-field model of the LTA process developed in EXCICO reproduces the process variability inherent to excimer lasers. The effect of different causes on laser shot (such as gas aging, gas mix, cavity pressure, cavity temperature, electrical discharge and the optical path quality) was translated in pulse duration and shape variation with deposited fluency.

We developed a model capable to simulate the LTA process for bulk c-Si based on Phase-Field approach and to simulate the dopant diffusion and segregation based on adsorption model within COMSOL Multiphysics. The simulated melt depths and melting times show a good agreement with those extracted from SIMS and in-situ reflectivity measurements, respectively. As for the boron diffusion and segregation model, the simulated Boron profiles show a fair agreement with the experimental SIMS profiles, considering an energy density instability within ±3%.

Since the model was calibrated for one layer bulk c-Si, multiple layers stack with different materials needs to be investigated and the model portability need to be validated. In the case of melting of materials other than Silicon, the model parameters will need to be adjusted, especially the phase field and the adsorption equations.

Finally, another objective of this study was to analyze the reliability of the process model. We have seen that it is possible to supply a tool to estimate non-measurable parameters needed for process optimization, process control and feasibility studies. The study aims primarily the application key requirement: the junction depth that is similar to the melt depth. But it could be developed for other types of targets such as an interface maximum temperature or a diffusion depth.

6. REFERENCES

[1] M. Hernandez, J. Venturini, D. Zahorski, et al., “Laser thermal processing for ultra shallow junction formation : numerical simulation and comparison with experiments”, Appl. Surf. Sci., vol. 208, p. 345, 2003

[2] T. Gutt, H. Schulze, T. Rupp, et al., “Laser Thermal Annealing for Power Field Effect Transistor by using Deep Melt Activation”, in RTP’06, p.193, 2006

[3] C. Sabatier, S. Rack, H. Beseaucele, et al., “Laser annealing of double implanted layers for IGBT Power Devices”, in RTP’08, p.177, 2008

[4] S.G. Wuu, C.C. Wang, D.N. Yaung, et al., “A manufacturable Back-Side Image Sensor”, in IEEE International Image Sensor Workshop, Bergen (Norway), 2009

[5] K. Huet, R. Lin, C. Boniface, et al., “Activation of ion implanted Si for backside processing by Ultra-fast Laser Thermal Annealing : Energy homogeneity and micro-scale sheet resistance”, in RTP’09, p.1, 2009

[6] H. Bourdon, A. Halimaoui, J. Venturini, et al., “Investigation of Excimer Laser Annealing of Si using Photoluminescence at Room Temperature”, in RTP’07, p. 275, 2007

[7] A. La Magna, G. Fortunato, M. Camalleri, B. Svensson, et al., “A phase-field approach to simulation of the excimer laser annealing process in Si”, J.App.Phy, vol. 95, no. 9, p. 4806, 2004

[8] M. Hackenberg, R. Negru, K. Huet, et al., “Modeling Boron profiles after pulsed excimer laser annealing”, in IIT 2012

[9] H. M. You, *et al.*, *J. Appl. Phys.* 74, 2461 (1993)

[10] F.A. Trumbore, *Bell. Syst. Tech. J.* 39, 205 (1960)
[11] Handbook Of Optical Materials, CRC Press LLC 2003
[12] K. Huet, G. Fisicaro, A. La Magna, et al, "Defect kinetics and dopant activation in sub microsecond laser thermal process", Appl. Phys. Lett. 95, 231901 (2009)